

Supplementary Data for Sittaramane et al.

One Table (Table S1)

11 figures with figure legends (Fig. S1 to S11)

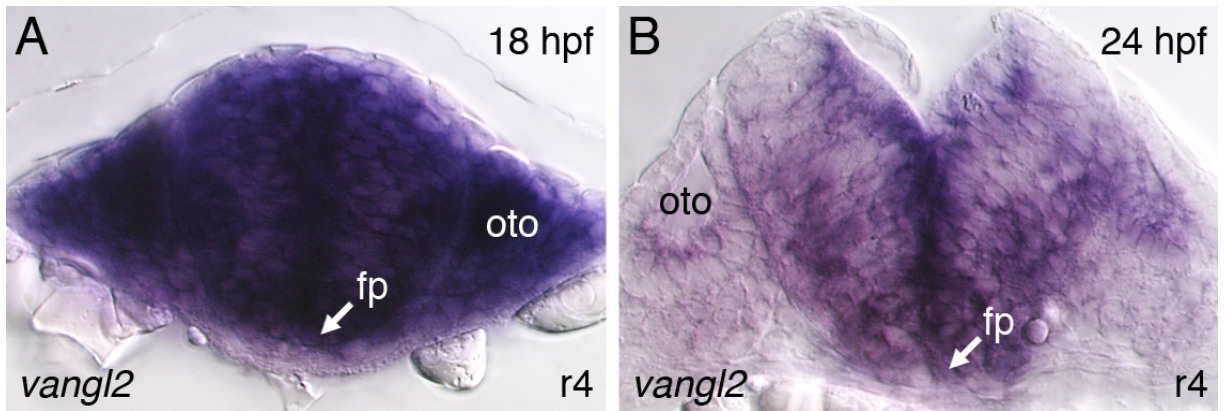
Table S1: Expression of Myc-Vangl2 in floor plate cells in r4 can efficiently rescue migration of FBM neurons in *vangl2*-deficient (*trilobite* mutant) embryos

	<i>trilobite</i> +/?; Tg(Fp:Gal4FF)+ve		<i>trilobite</i> +/?; Tg(Fp:Gal4FF)+ve		<i>trilobite</i> -/-; Tg(Fp:Gal4FF)+ve		<i>trilobite</i> -/-; Tg(Fp:Gal4FF)+ve	
	Tg(UAS: <i>vangl2</i>)+ve		Tg(UAS: <i>vangl2</i>)-ve		Tg(UAS: <i>vangl2</i>)+ve		Tg(UAS: <i>vangl2</i>)-ve	
Expt #	Do FBM neurons migrate out of r4?		Do FBM neurons migrate out of r4?		Do FBM neurons migrate out of r4?		Do FBM neurons migrate out of r4?	
	Yes	No	Yes	No	Yes*	No ^{&}	Yes	No
1	48	0	54	0	2	10	0	20
2	153	0	155	0	4	54	0	45
3	60	0	51	0	1	19	0	16
4	92	0	93	0	2	33	0	31
5	132	0	124	0	3	32	0	34
TOTAL	485	0	477	0	12*	148 ^{&}	0	146

*, Phenotypically mutant embryos (short trunks) containing FBM neurons migrating out of r4 were genotyped and confirmed as *tri*-/-. At least 50% of mutant neurons migrated out of r4 in every embryo (Figs. 3D and S8). In every embryo, MYC+ve (*Vangl2* +ve) floor plate cells were located in the r4 region (see summary data in Fig. 3F).

&, In these embryos, MYC+ve (*Vangl2* +ve) floor plate cells were located outside the r4 region (see summary data in Fig. 3F).

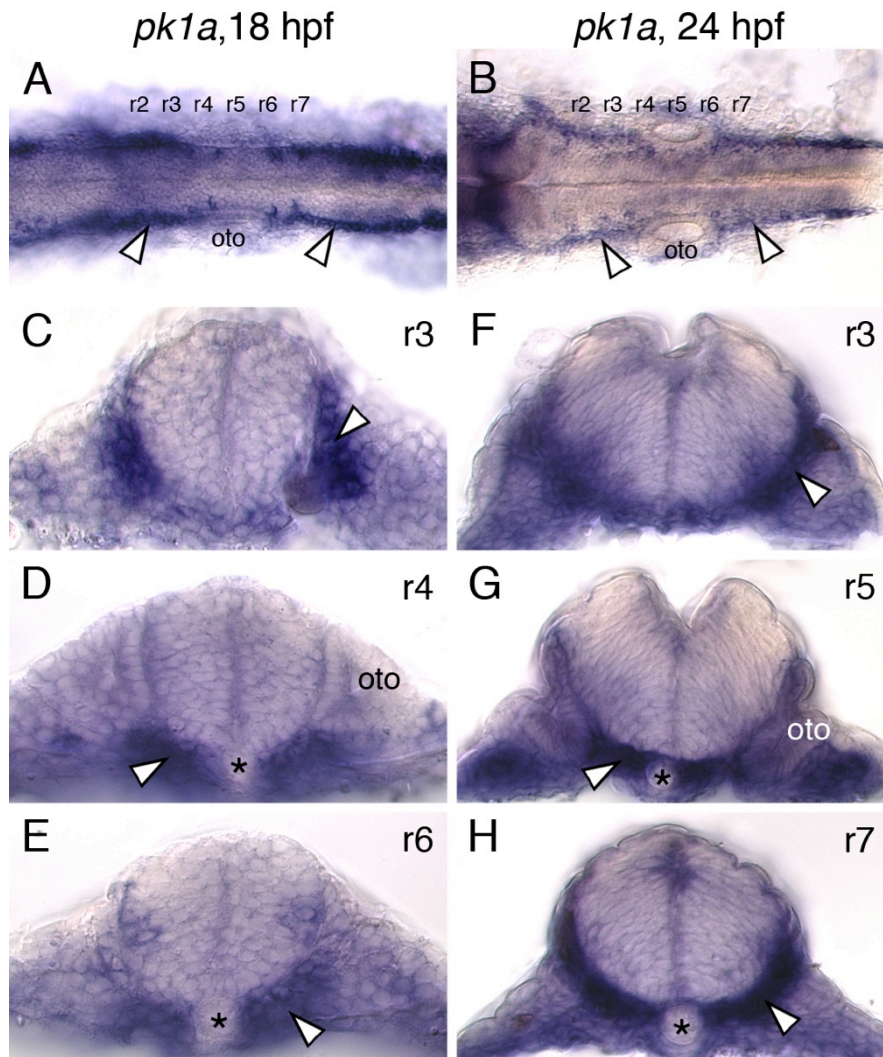
Figure S1



***Vangl2* is expressed broadly in the hindbrain and surrounding tissues during the period of FBM neuron migration.**

(A,B) Cross sections (30 microns thickness) in rhombomere 4 of 18 and 24 hpf zebrafish hindbrains processed for *vangl2* wholemount in situ (purple) reveals expression in the neural tube, and adjacent mesendoderm. fp, floor plate; oto, otocyst.

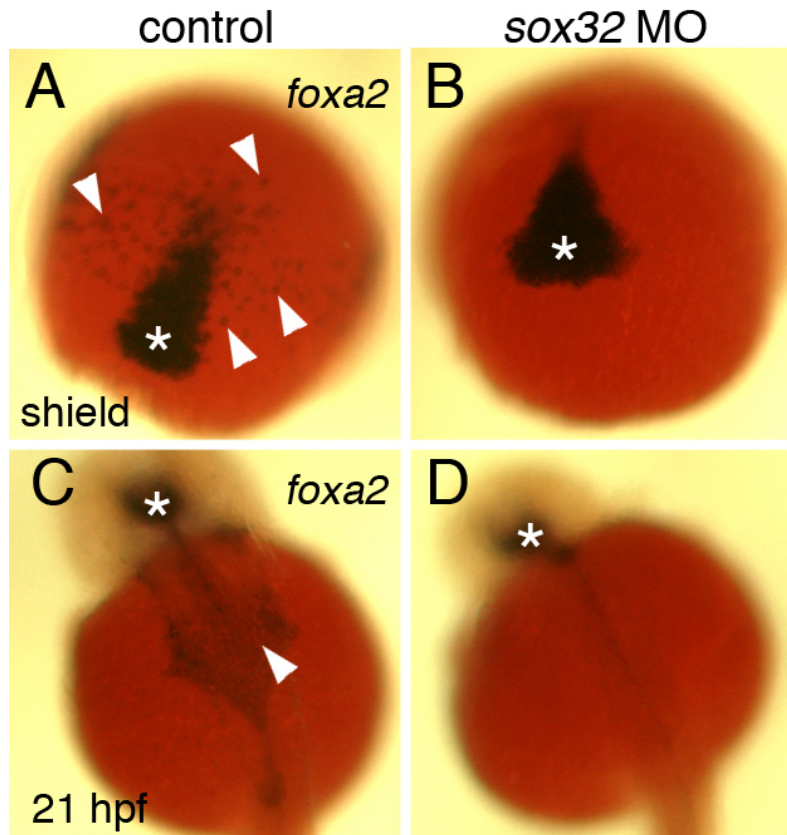
Figure S2



***pk1a* is expressed primarily outside the neural tube in the paraxial mesoderm and endoderm.**

(A,B) Dorsal views of zebrafish hindbrains at 18 and 24 hpf processed for *pk1a* in situ are suggestive of *pk1a* expression in the lateral regions of the neural tube (arrowheads). However, cross-sections at various levels through the hindbrain (C-H) reveal that *pk1a* is expressed primarily in the paraxial mesoderm and endoderm (arrowheads). Asterisks and oto indicate notochord and otic vesicle, respectively.

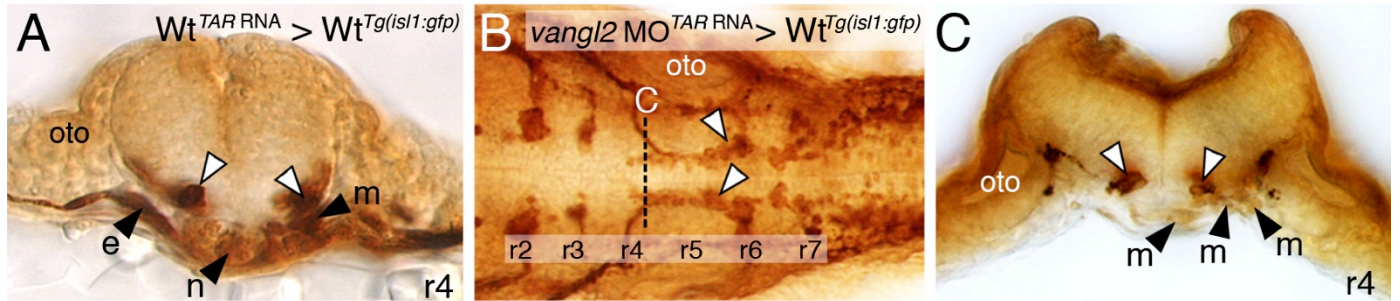
Figure S3



Absence of cranial endoderm in *sox32* morphants.

Dorsal views of control and *sox32* MO injected embryos processed for *foxa2* in situ to label endodermal cells (arrowheads) and axial mesoderm (asterisks). In *sox32* morphant embryos, endodermal cells are absent at both ages examined (**B,D**), whereas formation of axial mesoderm is not affected.

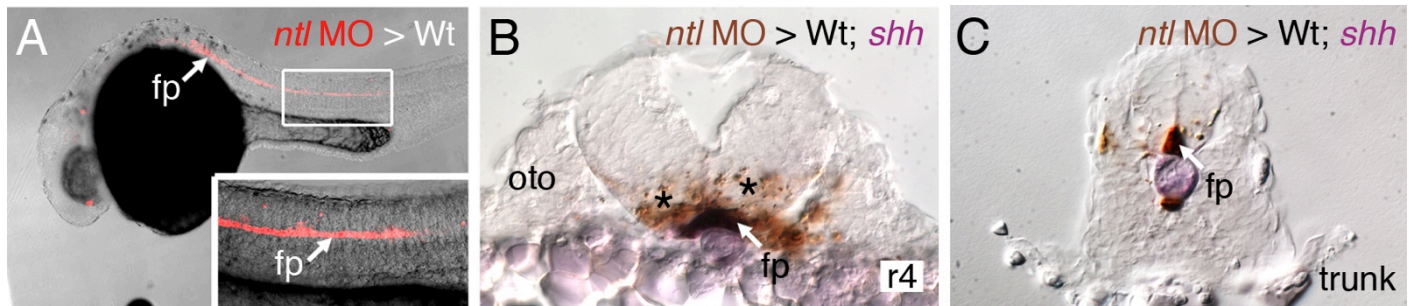
Figure S4



Mesodermal *vangl2* expression is not required for FBM neuron migration.

(A) Targeting of *TAR* RNA-injected donor cells to the endoderm and mesoderm in *Tg(isl1:GFP)* hosts. Hindbrain cross section at the r4 level in an 18 hpf host embryo stained for host FBM neurons (GFP antibody, white arrowheads) and donor-derived cells in the endoderm (e) and mesoderm (m), including the notochord (n) (staining of biotin-dextran in donor cells, black arrowheads). (B,C) Dorsal views of *Tg(isl1:GFP)* host hindbrain (B), with the level of r4 cross-section (C) indicated by the broken line. Targeting of *vangl2* morphant cells to the mesoderm (black arrowheads, C) in a wildtype host (B) does not have a significant effect on the migration of host neurons (white arrowheads in B, C). oto, otic vesicle.

Figure S5

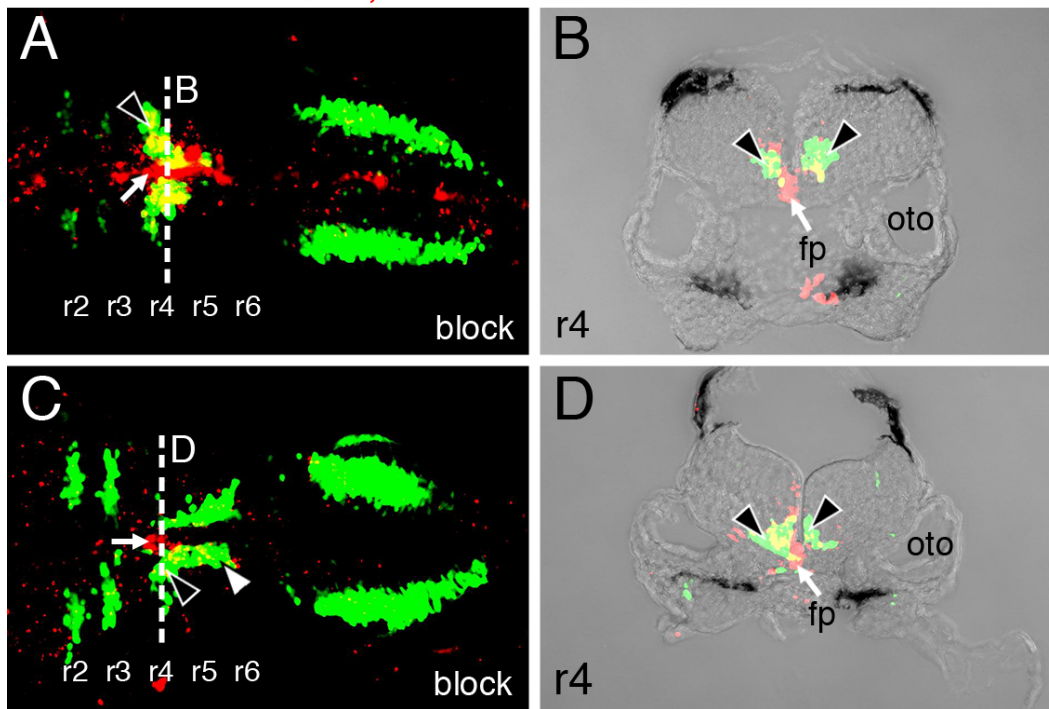


Targeting of transplanted donor cells to the floor plate of host embryos.

(A) Lateral view of a live 24 hpf wildtype embryo with donor-derived *no tail* (*ntl*) morphant cells (red, rhodamine and biotin dextran) in the floor plate. The embryo was then processed for *shh* in situ (purple) to label the floor plate and streptavidin immunochemistry (brown) to detect donor-derived cells. Cross sections at the r4 (B) and trunk (C) levels show the presence of donor cells (arrows) in the floor plate. oto, otic vesicle. Asterisks in B indicate labeled cell debris from the transplantation procedure.

Figure S6

tri^{-/-}, *ntl* MO > Wt *Tg(isl1:gfp)*

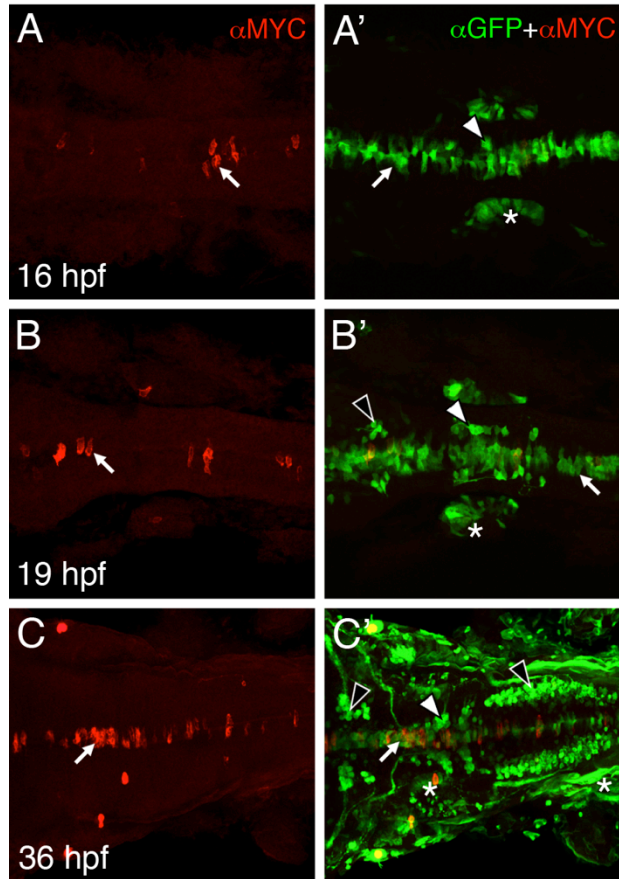


Presence of *vangl2* mutant floor plate cells in r4 can block the migration of wildtype FBM neurons.

(A,C) Dorsal views of the hindbrain of wildtype *Tg(isl1:GFP)* embryos with donor-derived *vangl2* mutant (*tri*^{-/-}) cells in the floor plate (red, arrows). Presence of mutant cells in the host floor plate can block the migration of wildtype FBM neurons out of r4 (black arrowheads). Many FBM neurons (white arrowhead) migrate normally. (B,D) Cross-sections of the embryos at the r4 level (broken lines in A,C) show the presence of donor-derived floor plate cells (red, arrows) and non-migrated host FBM neurons (arrowheads). The yellow signals in the merged images are largely debris associated with transplantation or artifacts of superimposition of signals in different slices following stacking of confocal images. We verified that *ntl* morphant cells do not differentiate into FBM neurons (see Materials and Methods). oto, otic vesicle; fp, floor plate.

Figure S7

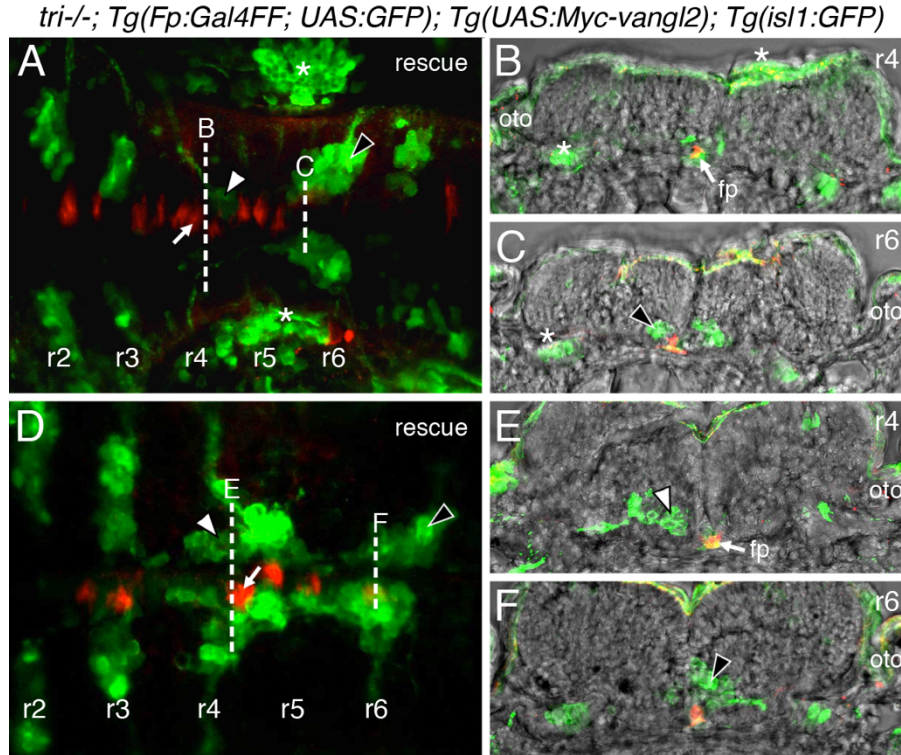
Tg(Fp:Gal4FF; UAS:GFP);
Tg(UAS:Myc-vangl2); Tg(isl1:GFP)



***Tg(Fp:Gal4FF)* and *Tg(UAS:Myc-vangl2)* transgenes induce mosaic expression of Myc-Vangl2 in the floor plate.**

(A-C') Dorsal views of the hindbrain in *Tg(Fp:Gal4FF); Tg(UAS:GFP); Tg(UAS:Myc-vangl2); Tg(isl1:GFP)* embryos stained with anti-MYC antibody to label Myc-Vangl2-expressing cells (A-C, red) and anti-GFP antibody to label *UAS:GFP*-expressing cells and *isl1:GFP*-expressing branchiomotor neurons (A'-C', green). The *UAS:GFP* transgene is expressed at all ages in floor plate cells (A'-C', arrows). Gal4FF induces mosaic expression of the *UAS:Myc-Vangl2* transgene in the floor plate (A-C, arrows). The *isl1:GFP* transgene is expressed in FBM neurons (A'-C', white arrowheads), and in the trigeminal and vagal motor neurons (B',C', black arrowheads). Asterisks (A'-C') indicate Gal4FF-driven expression of the *UAS:GFP* transgene in the otic vesicle, trunk muscles, and skin. The Gal4FF driver does not induce *UAS:GFP* expression in branchiomotor neurons.

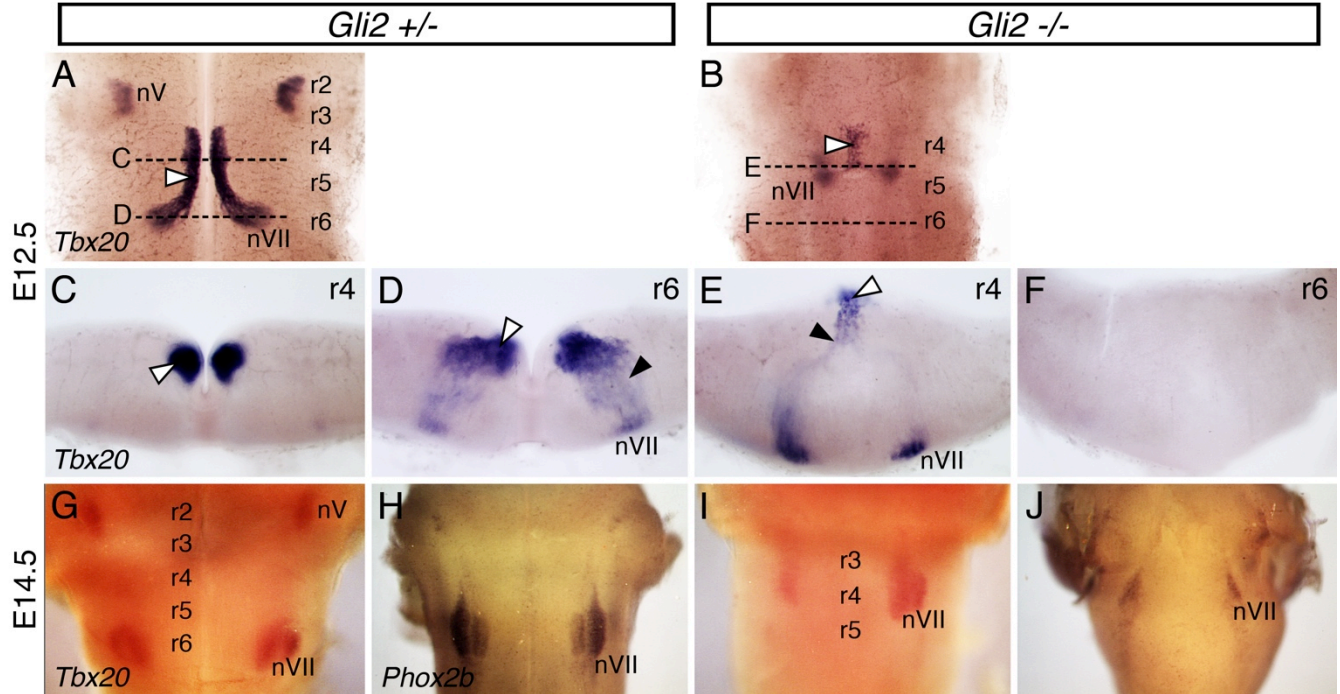
Figure S8



Expression of *vangl2* transgene in floor plate cells can rescue FBM neuron migration in *vangl2* (*tri*^{-/-}) mutants.

(A,D) Dorsal views of the hindbrain of *tri*^{-/-}; *Tg(Fp:Gal4FF; UAS:GFP)*; *Tg(UAS:Myc-vangl2)*; *Tg(isl1:GFP)* embryos immunostained with anti-MYC antibody (red) and anti-GFP antibody (green). Presence of Myc-Vangl2-expressing floor plate cells in r4 (arrows) effectively rescues the migration of *vangl2* mutant FBM neurons (A and D, black arrowheads). (B,C) Cross sections of the embryo in A at the indicated levels showing Myc-Vangl2 expression in the floor plate (B, arrow) and migrated *vangl2* mutant FBM neurons in r6 (C, black arrowhead). (E,F) Cross sections of the embryo in D at the indicated levels showing Myc-Vangl2 expression in the floor plate (E, arrow) and migrated *vangl2* mutant FBM neurons in r6 (F, black arrowhead). Non-migrated neurons (white arrowheads) are seen in D and E. Floor plate cells are yellow due to GFP expression from the *UAS:GFP* transgene. Asterisks indicate Gal4FF-driven expression of the *UAS:GFP* transgene in otic vesicle and skin. The Gal4FF driver does not induce *UAS:GFP* expression in branchiomotor neurons. oto, otic vesicle; fp, floor plate.

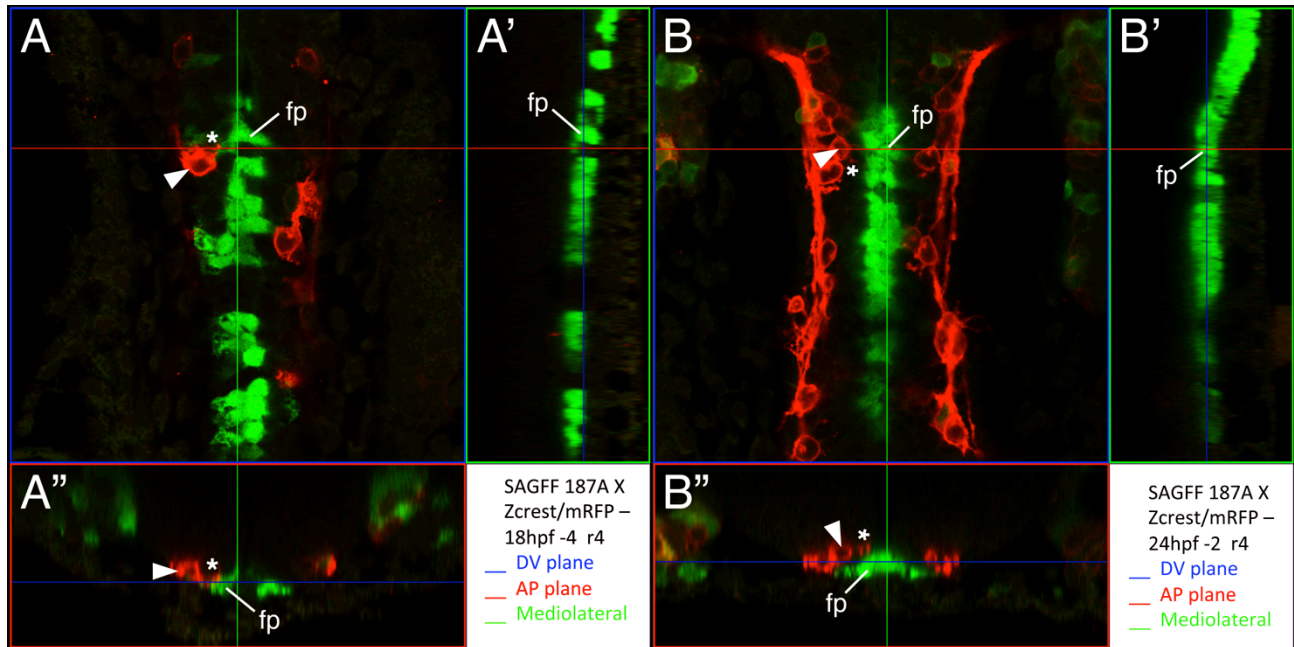
Figure S9



FBM neurons fail to migrate caudally in mouse *Gli2* mutants lacking a floor plate.

(A,B) Dorsal views of mouse hindbrain at E12.5 processed for *Tbx20* in situ. C-F depict cross sections at the indicated levels (broken lines). In a *Gli2*^{+/-} embryo (A,C,D), FBM neurons migrate caudally from r4 into r6 (A and C, white arrowheads), then undergo radial migration to the pial surface of the neural tube in r6 (D, black arrowhead). In a *Gli2*^{-/-} embryo (B,E,F), FBM neurons are found in a single cluster (B and E, white arrowheads) at the midline and fail to migrate caudally out of r4. However, some FBM neurons undergo radial migration to the pial surface of the neural tube in r4 (E, black arrowhead). (G-J) Dorsal views of E14.5 hindbrains processed for *Tbx20* (G,I) or *Phox2b* (H,J) in situs. In *Gli2*^{+/-} embryos (G, H; n=3 for each probe), the facial motor nuclei (nVII, FMN) are located at the pial surface of r6. In *Gli2*^{-/-} (I,J; n=3 for each probe), the FMN are displaced rostrally and reduced in size.

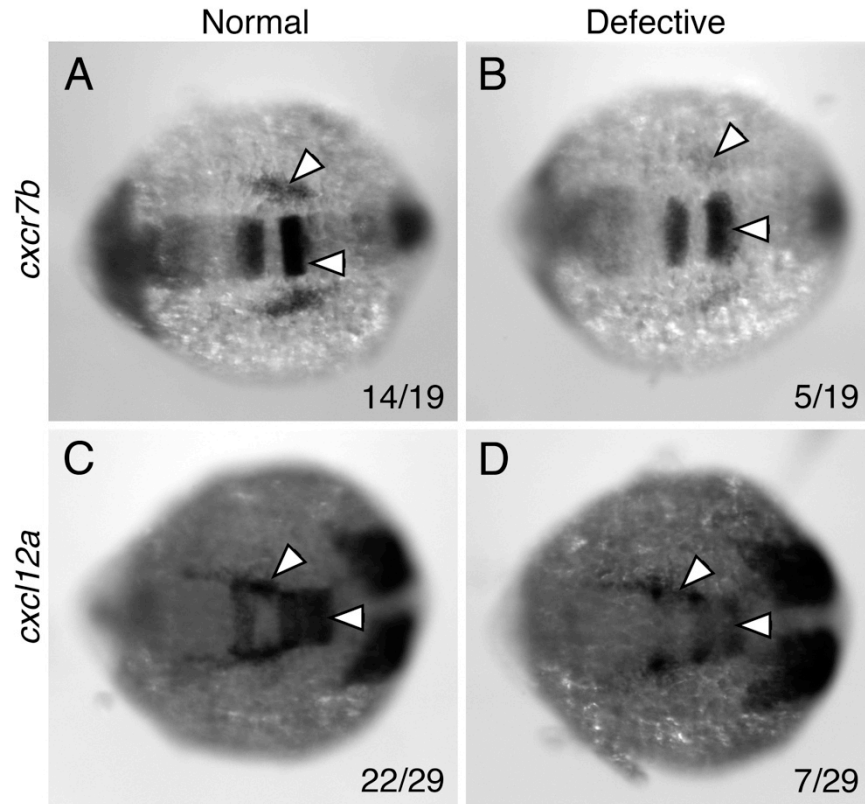
Figure S10



Some FBM neuron protrusions contact floor plate cells

Confocal projection views of the hindbrain of *SAGFF187A aka Tg(Fp:Gal4FF); Tg(UAS:GFP); Tg(zCREST:mRFP)* embryos stained with anti-RFP antibody to label FBM neurons (red) and anti-GFP antibody to label *UAS:GFP*-expressing cells (green). (**A,B**) Dorsal views at the levels indicated by blue lines in **A''** and **B''**. Protrusions (asterisks) from FBM neurons (arrowheads) are very close to or in contact with floor plate cells (fp). (**A',B'**) Sagittal views (mediolateral projections) at the levels indicated by green lines in **A** and **B**. (**A'',B''**) Cross-sectional views at the anterior-posterior levels indicated by red lines in **A** and **B**. The protrusions from FBM neurons are touching or in apposition to the floor plate cells. We restricted our analysis to FBM neurons located in r4/r5, and found that 34/52 protrusions (44 neurons in 8 embryos) contacted floor plate cells.

Figure S11



Aberrant chemokine gene expression in putative *detour* mutants

(A-D) Dorsal views of the hindbrain region, with anterior to left, in 7-somite stage embryos obtained from a *detour te370a/+* incross, processed for in situ hybridization with *cxcr7b* (A,B) or *cxcl12a* (C,D). Whereas most embryos (A,C) showed normal expression of these genes in the hindbrain and sensory neurons (arrowheads), some (B,D) exhibited defects (arrowheads). However, sequencing of the *gli1* locus that is mutated in the *dtr te370a* allele did not show linkage between the defective phenotype and the *dtr*^{-/-} genotype. Nonetheless, it remains formally possible that inefficient migration of FBM neurons in *detour* mutants results from reduced chemokine signaling.